# **Electrochemical Sensor Based on Graphene Oxide/Iron Nanoparticles for the Analysis of Quercetin**

*Onur Akyıldırım<sup>1</sup>, Hilal Medetalibeyoğlu<sup>2</sup>, Sevda Manap<sup>2</sup>, Murat Beytur<sup>2</sup>, Feyzi Sinan Tokalı<sup>2</sup>, Mehmet Lütfi Yola<sup>3,\*</sup>, Necip Atar<sup>4,\*</sup>* 

<sup>1</sup> Department of Chemical Engineering, Faculty of Engineering and Architecture, Kafkas University, Kars, Turkey
 <sup>2</sup> Department of Chemistry, Faculty of Science and Letters, Kafkas University, Kars, Turkey
 <sup>3</sup> Department of Metallurgical and Materials Engineering, Faculty of Engineering, Sinop University, Sinop, Turkey
 <sup>4</sup> Department of Chemical Engineering, Faculty of Engineering, Pamukkale University, Denizli, Turkey
 \*E-mail: <a href="mailto:necipatar@gmail.com">necipatar@gmail.com</a>; mehmetyola@gmail.com

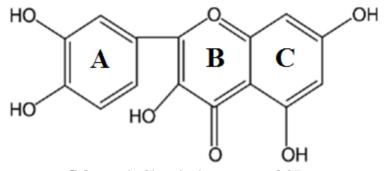
Received: 18 May 2015 / Accepted: 18 June 2015 / Published: 28 July 2015

We aimed a novel electrochemical sensor based on iron nanoparticles (FeNPs) and 2-aminoethanethiol (2-AET) functionalized graphene oxide (2-AETGO). The methods such as transmission electron microscope (TEM), scanning electron microscope (SEM), x-ray photoelectron spectroscopy (XPS), reflection–absorption infrared spectroscopy (RAIRS), electrochemical impedance spectroscopy (EIS) and the x-ray diffraction (XRD) method were used for the characterizations of nanocomposites. The linearity and the detection limit of quercetin (QR) were  $1.0 \times 10^{-8} - 1.0 \times 10^{-7}$  M and  $2.0 \times 10^{-9}$  M, respectively. The modified glassy carbon electrode (FeNPs/2-AETGO/GCE) was applied to the determination of QR in food sample such as apple juice.

Keywords: quercetin, graphene oxide, iron nanoparticles, characterization

## **1. INTRODUCTION**

QR is flavonoid and some fruits and vegetables have flavonoids such as quercetin, morin, rutin [1, 2]. The structure of QR is seen in Scheme 1. In addition, QR has important properties such as anti-inflammatory and antioxidant [3].



Scheme 1. Chemical structure of QR

Especially, various nanomaterials, nanofilms and nanoparticles can been used for the development of sensitive method in nanotechnology [4-8]. In addition, significant progress has been performed in the production of carbon-supported materials in the development of nanosensor [9, 10]. Nevertheless, there are some important problems such as low catalytic performance for analysis. Hence, in order to increase this performance, the novel nanomaterials such as graphene/graphene oxide (GO) and carbon nanotubes become very significant [11, 12]. In addition, some nanoparticles such as mono/bimetallic attracted important attention in nano/sensor technology. Because the nano-sized particles have larger specific surface area, they are good catalysts. The nanoparticles can also increase the rate of electrochemical reaction [13]. The important sensor development in nanotechnology has been considered as great tool [7, 14-26]. Because of these properties, the sensitive determination of important drugs in food samples is very necessary. In addition, nanocatalytic studies based on nanocomposites have been reported in terms of development of catalytic effect [5, 27-30].

Some analytical tecniques have been studied for analysis of QR, including chromatography, spectrophotometry and capillary electrophoresis [31, 32]. However these tecniques have some negative effects such as large expensive equipment. We aimed to develop a sensitive voltammetric sensor based on FeNPs/2-AET/GO nanocomposite in present study. In addition, the selectivity and stability properties of developed sensor are reported.

## 2. EXPERIMENTAL

#### 2.1. Materials

QR was obtained from Sigma–Aldrich. The stock solutions of QR (1.0 mM) were prepared by ethanol and the stock solution was diluted with phosphate buffer solution (PBS) (pH 6). Graphite powder, 2-AET, iron nitrate (FeNO<sub>3</sub>), 1-ethyl-3-[3-dimethylaminopropyl] carbodiimide hydrochloride (EDC), MeCN, ethanol, isopropyl alcohol (IPA), hydrogen peroxide (H<sub>2</sub>O<sub>2</sub>), potassium permanganate (KMnO<sub>4</sub>), sulphuric acid (H<sub>2</sub>SO<sub>4</sub>) and activated carbon were purchased from Sigma–Aldrich (USA). Potassium persulfate (K<sub>2</sub>S<sub>2</sub>O<sub>8</sub>) and phosphorus pentoxide (P<sub>2</sub>O<sub>5</sub>) were bought from Merck (Germany).

## 2.2. Instrumentation

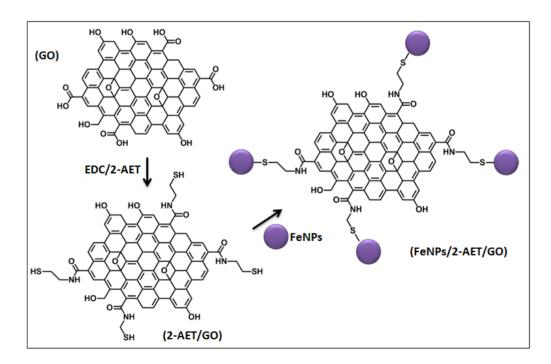
Square wave voltammetry (SWV) and cyclic voltammetry (CV) were carried out IviumStat (U.S) equipped with C3 cell stand. Electrochemical impedance spectroscopic experiments were carried out with IVIUMSTAT & IVIUMSTAT.XR: Electrochemical Interface & Impedance Analyser. PHI 5000 Versa Probe ( $\Phi$  ULVAC-PHI, Inc., Japan/USA) was utilized for XPS analysis with monochromatized Al K $\alpha$  radiation (1486.6 eV) as an x-ray anode operated at 50 W. TEM images were obtained on a JEOL 2100 HRTEM instrument (JEOL Ltd., Tokyo, Japan) and a SEM is ZEISS EVO 50 analytic microscope (Germany). A Rigaku Mini X-ray diffractometer was used for X-ray diffraction measurements. The RAIRS measurements of the nanocomposites were recorded with Bruker Tensor 27 FT-IR DTGS detector by using a Ge total reflection accessory.

## 2.3. Synthesis of GO

GO was synthesized according to our previous report [12]. The GO suspension was interacted with 0.2 M EDC solution for 8 h to activate carboxylate groups. Activated GO suspension was mixed well with 1.0 mM 2-AET at a 1:1 volume ratio for 2 h (2-AETGO).

## 2.4. Synthesis of FeNPs/2-AET/GO

FeNPs was synthesized according to our previous report [13]. FeNPs (2 mg mL<sup>-1</sup>) was mixed with the dispersion of 2-AETGO nano-sheets (0.2 mg mL<sup>-1</sup>) at a 1:1 volume ratio (FeNPs/2-AETGO). The structure of the synthesized FeNPs/2-AETGO nanocomposite is demonstrated in Scheme 2.



Scheme 2. The structure of FeNPs/2-AETGO nanocomposite

## 2.5. Procedure for the electrode preparation

GCE was cleaned according to our previous reports [18, 19]. After that, 15  $\mu$ L of FeNPs/2-AETGO suspensions was dropped onto the clean GCE.

#### 2.6. Sample preparation

The samples of apple juice were bought from a supermarket in Sinop/TURKEY. The samples were filtered with a 0.10  $\mu$ m filter. The values of pH for samples were adjusted using 0.1 M PBS. The experiments of selectivity were performed according to the protocol: Firstly, the calibration and standard addition methods were applied to the apple juice samples. The difference between slopes of calibration and standard addition curves was evaluated. In addition, the recovery experiments were carried out in apple juice samples and the values of recovery were evaluated.

## **3. RESULTS AND DISCUSSION**

#### 3.1. Characterizations of FeNPs/2-AETGO composite

The RAIRS spectrum reveals the very characteristic stretching vibrations of C=O (–COOH) (1715 cm<sup>-1</sup>) and O–H (–COOH) (3520 cm<sup>-1</sup>) on the edges of GO (Fig. 1). Fig. 1 confirms the presence of covalently attached 2-AET on graphene oxide. The peaks at 1640 cm<sup>-1</sup> and 1370 cm<sup>-1</sup> are attributed to aromatic C=C double bond stretching and C–H bending vibrational frequencies in graphene oxide, respectively. In addition, the existence of the band at 3350 cm<sup>-1</sup> for the N–H stretching vibration bond confirms the covalent functionalization of the carboxyl group of the functionalized graphene oxide with 2-AET [33].

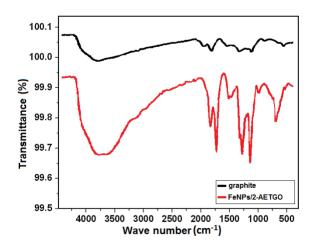


Figure 1. RAIRS spectra of the graphite and FeNPs/2-AETGO nanocomposite

The TEM image (Fig. 2A) of the GO demonstrated GO nano-sheets such as few-layer planar. The spherical shapes of FeNPs have been seen on GO nano-sheets (Fig. 2B). Figure 2B indicates uniformly distribution of FeNPs with a mean diameter of 15-25 nm.

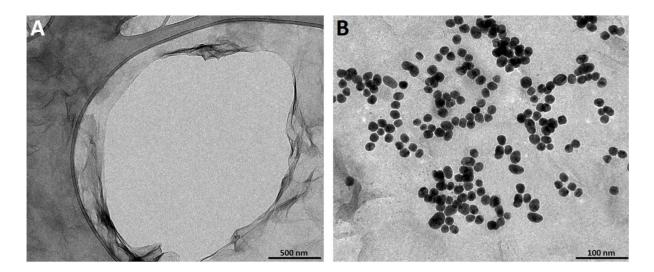


Figure 2. TEM images of (A) GO, (B) FeNPs/2-AETGO

The SEM characterization is used to investigate the morphologies of the surfaces. Fig. 3A shows the smooth surface of the bare GCE. To show the modification of GCE with 2-AETGO, some layers were observed on the 2-AETGO/GCE surface in Fig. 3B. After modification of FeNPs on the 2-AETGO/GCE, an intensive layer of FeNPs was covered on the 2-AETGO modified GCE (Fig. 3B).

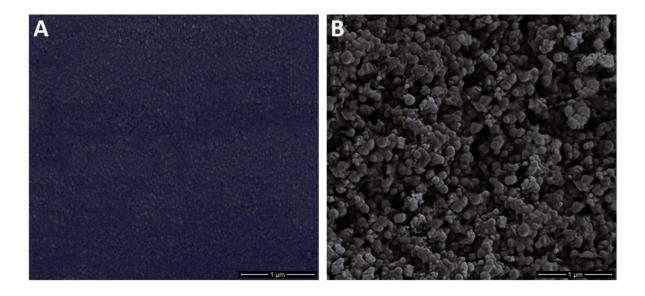


Figure 3. SEM images of (A) bare GCE, (B) FeNPs/2-AETGO modified GCE

The formation of FeNPs/2-AETGO was examined by XPS. The peaks of C1s, N1s, S2p and Fe2p prove the formation of FeNPs/2-AETGO nanocomposite (Fig. 4). The peaks at 283.4 eV, 284.9 eV and 286.2 eV were corresponded to C-H, C-N and –CONH of C1s core-level spectrum,

respectively [1] (Fig. 4A). N1s narrow region spectrum was curve-fitted and the peak observed at 397.9 eV was corresponded to the N–H groups of amide. The unreacted N-H groups of 2-AET was shown at 401.1 eV (Fig. 4B). S2p zone was curve-fitted with two components by a doublet 2p1/2 and 2p3/2 signals [1]. The peak at 164.9 eV confirmed the presence of iron nanoparticles grafted to S atom. The unreacted thiol group of 2-AET has been shown at 162.6 eV (Fig. 4C). The Fe2p peaks confirm the presence of Fe bonded [1] (Fig. 4D).

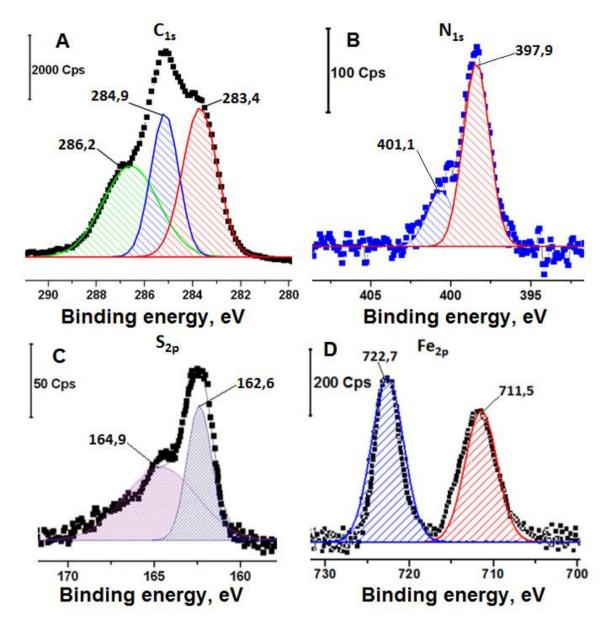


Figure 4. The narrow region XPS spectra of FeNPs/2-AETGO nanocomposite for the deconvolution spectra of the (A)  $C_{1s}$ , (B)  $N_{1s}$ , (C)  $S_{2p}$  and (D)  $Fe_{2p}$ 

Fig. 5 shows the XRD patterns of the nanocomposite. the XRD patterns show the weak peaks at  $2\theta = 32.1^{\circ}$  and  $2\theta = 44.5^{\circ}$  were corresponded to (101) and (004) planes of GO layers, respectively. The other peaks indicate the formation of Fe°[4].

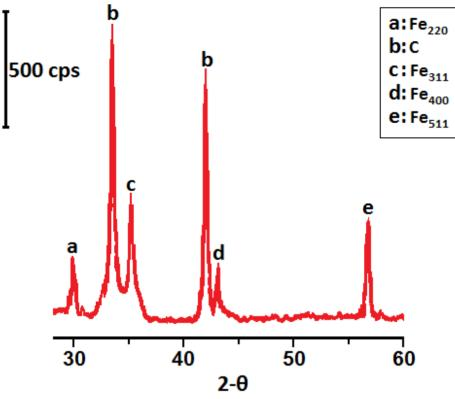


Figure 5. XRD patterns of the FeNPs/2-AETGO nanocomposite

### 3.2. Cyclic voltammograms and EIS studies of QR at modified electrodes

Fig. 6 demonstrated the cyclic voltammograms of  $1.0 \times 10^{-3}$  M QR in 0.1 M PBS (pH 6.0) at modified electrodes. The anodic and cathodic currents at the FeNPs/2-AETGO modified GCE were higher than those at others while the peak potentials at the modified electrodes are the same. The high catalytic effect indicated that GO and FeNPs accelerated the rate of electron transfer and surface area [2].

The pH effect on the peak potential was studied. The slope of the  $E_p$ -pH plot was -58.7 mV/pH for the FeNPs/2-AET/GO modified GCE. According to the results, equal numbers of electrons and protons are occurred at the modified surface. Among the hydroxyl groups of QR, the catechol dihydroxyl electron-donating group (ring A) with the highest level of electroactivity may be oxidized at low potentials and show high peak currents [33]. The plots of log  $I_{pa}$  vs. log v and log  $I_{pc}$  vs. log v in the range of 50-1000 mV s<sup>-1</sup> are 0.491 and 0.509, respectively. We can say that the electrochemical process is diffusion-controlled. The relationship of the redox peak potentials with the logarithm of scan rate was also obtained with the linear regression equations as  $E_{pa} = 0.147 + 0.0159 \ln v$  ( $E_{pa}$ : V, v: V s<sup>-1</sup>, R<sup>2</sup>: 0.9991) and  $E_{pc} = 0.127 - 0.0141 \ln v$  ( $E_{pc}$ : V, v: V s<sup>-1</sup>, R<sup>2</sup>: 0.9987), respectively. Based on the following equations [34].

$$E_{pa} = E_0 + m[0.78 + ln(D^{1/2}k_s^{-1}) - 0.5lnm] + (m/2)lnv, \quad m = RT/(1-\alpha)nF$$
(1)

$$E_{pc} = E_0' - m' [0.78 + ln(D^{1/2}k_s^{-1}) - 0.5lnm'] - (m'/2)lnv, \quad m' = RT/\alpha nF$$
(2)

the electron-transfer coefficient ( $\alpha$ ) is calculated as 0.497 for three measurements.

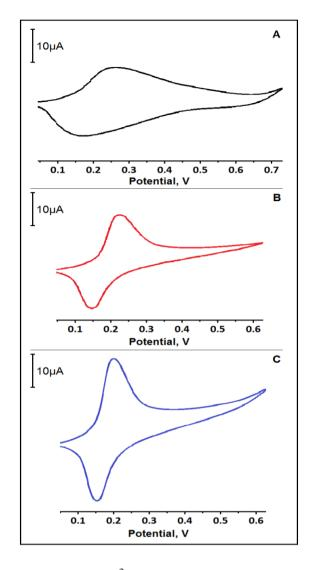


**Figure 6.** Cyclic voltammograms of  $1.0 \times 10^{-3}$  M QR in 0.1 M PBS (pH 6.0) (a) at bare GCE, (b) GO modified GCE, (c) FeNPs/2-AETGO modified GCE (Scan rate is 100 mV s<sup>-1</sup>)

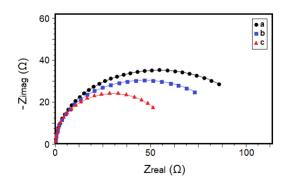


**Figure 7.** Impedance spectrum for 1.0 mM [Fe(CN)<sub>6</sub>]<sup>3-/4-</sup> (1:1) in 0.1 M KCl at (a) GCE, (b) GO modified GCE and (c) FeNPs/2-AETGO modified GCE surfaces

Fig. 7 shows the impedance plot of (a) GCE, (b) GO modified GCE and (c) FeNPs/2-AETGO modified GCE in 1.0 mM  $[Fe(CN)_6]^{3-/4-}$  (1:1) solution in 0.1 M KCl. The values of charge transfer

resistance ( $R_{ct}$ ) were calculated for at bare GCE, the GO modified GCE and FeNPs/2-AETGO modified GCE as 110.0  $\Omega$ , 95.0  $\Omega$  and 60.0  $\Omega$ , respectively. The value of  $R_{ct}$  at the FeNPs/2-AETGO modified GCE is lower than those at the other surfaces. Hence, the preparation of FeNPs functionalized 2-AETGO leads to accelerate the transfer of the electrons.

## 3.3. Analytical application

## 3.3.1. Linearity range of voltammetric sensor

The voltammograms with concentrations of QR (Fig. 8) show that the signals are linear with amount of QR. The regression graph was related to the mean value of six measurements. The calibration equation of OCH (Fig. 8B) is y ( $\mu$ A) = 64.098x ( $\mu$ M) + 0.7459. Limit of quantification (LOQ) and limit of detection (LOD) for QR were obtained as  $1.0 \times 10^{-8}$  M and  $2.0 \times 10^{-9}$  M, respectively [35, 36].

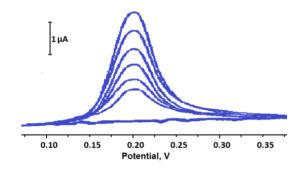


**Figure 8.** (A) Effect of concentration on the peak current of QR at the FeNPs/2-AETGO modified GCE (a) 0.1 M PBS (pH 6.0), (b)  $1.0 \times 10^{-8}$ , (c)  $2.0 \times 10^{-8}$ , (d)  $3.0 \times 10^{-8}$ , (e)  $4.0 \times 10^{-8}$ , (f)  $5.0 \times 10^{-8}$ , (g)  $1.0 \times 10^{-7}$  M QR, which was registered by the FeNPs/2-AETGO modified GCE

## 3.3.2. Recovery

In addition, the recovery experiments were carried out in apple juice samples. According to Table 1, the values of recovery are close to 100.00%. Thus, we can say that the ingredients in the real samples did not affect the performance of the developed voltammetric sensor.

	<b>Table 1.</b> The recovery	of QR in	apple juice	samples (n=7)
--	------------------------------	----------	-------------	---------------

Sample	Added QR (M)	Found QR (M)	Recovery (%)
Apple	-	$2.10\pm(0.02)\times10^{-8}$	-
juice	2.0×10 <sup>-8</sup>	$4.00(\pm 0.05) \times 10^{-8}$	$97.56 \pm 0.9$
	3.0×10 <sup>-8</sup>	$5.07(\pm 0.02) \times 10^{-8}$	$99.41 \pm 1.0$
	$4.0 \times 10^{-8}$	$6.05(\pm 0.05) \times 10^{-8}$	99.18 ± 1.6

## 3.3.3. Selectivity and Stability of the voltammetric sensor

The standard addition technique was applied to the apple juice samples. The regression equation was y ( $\mu$ A) = 63.071x ( $\mu$ M) + 10.7148 for QR. According to the results, there was no interference from matrix components. The stability of one FeNPs/2-AETGO modified GCE was investigated. After 30 days, the signal is 99.14% of the original peak current. This stability shows that FeNPs/2-AETGO modified GCE can be used in long-term for determination of QR. A rapid, simple and sensitive LC–MS/MS method was employed as a comparison to evaluate the validity of the developed method. Table 2 gives the results obtained by the two methods for the determination of QR in apple juice samples. These results were compared by Wilcoxon test and there was no significant difference between the obtained results of SWV and LC–MS/MS (Tcalculated > Ttabulated, p > 0.05).

**Table 2.** Comparison of the results obtained by SWV and LC–MS/MS methods for determination of QR (n = 6)

	Foun	Found QR		
Sample	SWV	LC-MS/MS		
Apple juice (M)	2.10±(0.02)×10 <sup>-8</sup>	2.12±(0.04)×10 <sup>-8</sup>		
SD	0.02	0.02		
RSD	0.95	0.94		

 $\overline{X}$ : Mean ± Standard Error, SD: Standard Deviation, RSD: % Relative Standard Deviation

## 4. CONCLUSIONS

A electrochemical sensor based on FeNPs involved in 2-AETGO was developed for analysis of QR in apple juice. The nanomaterials were characterized well by several methods. The voltammetric sensor demonstrated selectivity and sensitivity towards QR with a detection limit of  $2.0 \times 10^{-9}$  M. In addition, the developed sensor is stable in long-term. The prepared voltammetric sensor has potential to be applied to the routine analysis of QR in food samples.

### References

- 1. M.L. Yola, T. Eren, N. Atar, Biosensors and Bioelectronics 60 (2014) 277.
- M.L. Yola, N. Atar, Z. Üstündağ, A.O. Solak, *Journal of Electroanalytical Chemistry* 698 (2013)
   9.
- 3. M.L. Yola, V.K. Gupta, T. Eren, A.E. Şen, N. Atar, *Electrochimica Acta* 120 (2014) 204.
- 4. M.L. Yola, T. Eren, N. Atar, *Electrochimica Acta* 125 (2014) 38.
- 5. M.L. Yola, T. Eren, N. Atar, *Chemical Engineering Journal* 250 (2014) 288.
- 6. M.L. Yola, T. Eren, N. Atar, S. Wang, Chemical Engineering Journal 242 (2014) 333.
- M.L. Yola, T. Eren, H. Ilkimen, N. Atar, C. Yenikaya, *Journal of Molecular Liquids* 197 (2014) 58.
- 8. V.K. Gupta, M.L. Yola, N. Atar, Z. Üstündağ, A.O. Solak, *Journal of Molecular Liquids* 191 (2014) 172.
- 9. V.K. Gupta, M.L. Yola, N. Atar, Z. Ustundagì, A.O. Solak, *Electrochimica Acta* 112 (2013) 541.

- 10. V.K. Gupta, N. Atar, M.L. Yola, M. Eryilmaz, H. Torul, U. Tamer, T.H. Boyaci, Z. Üstündağ, Journal of Colloid and Interface Science 406 (2013) 231.
- 11. M.L. Yola, T. Eren, N. Atar, Biosensors & Bioelectronics 60 (2014) 277.
- 12. M.L. Yola, T. Eren, N. Atar, Sensors and Actuators, B: Chemical 210 (2015) 149.
- 13. V.K. Gupta, N. Atar, M.L. Yola, Z. Üstündağ, L. Uzun, Water Research 48 (2014) 210.
- 14. M.L. Yola, T. Eren, N. Atar, Sensors and Actuators, B: Chemical 195 (2014) 28.
- 15. M.L. Yola, N. Atar, T. Eren, Sensors and Actuators, B: Chemical 198 (2014) 70.
- V.K. Gupta, M.L. Yola, N. Atar, A.O. Solak, L. Uzun, Z. Üstündağ, *Electrochimica Acta* 105 (2013) 149.
- 17. V.K. Gupta, M.L. Yola, N. Atar, Sensors and Actuators, B: Chemical 194 (2014) 79.
- V.K. Gupta, M.L. Yola, N. Özaltin, N. Atar, Z. Üstündağ, L. Uzun, *Electrochimica Acta 1*12 (2013) 37.
- 19. M.L. Yola, N. Atar, M.S. Qureshi, Z. Üstündag, A.O. Solak, Sensors and Actuators, B: Chemical 171-172 (2012) 1207.
- 20. V.K. Gupta, M.L. Yola, M.S. Qureshi, A.O. Solak, N. Atar, Z. Üstündağ, Sensors and Actuators, B: Chemical 188 (2013) 1201.
- 21. N. Atar, T. Eren, M.L. Yola, Food Chemistry 184 (2015) 7.
- 22. T. Eren, N. Atar, M.L. Yola, H. Karimi-Maleh, Food Chemistry 185 (2015) 430.
- 23. H. Karimi-Maleh, F. Tahernejad-Javazmi, N. Atar, M.L. Yola, V.K. Gupta, A.A. Ensafi, *Industrial* and Engineering Chemistry Research 54 (2015) 3634.
- 24. M.L. Yola, L. Uzun, N. Özaltin, A. Denizli, Talanta 120 (2014) 318.
- 25. N. Atar, T. Eren, M.L. Yola, S. Wang, Sensors and Actuators B: Chemical 216 (2015) 638.
- 26. V.K. Gupta, M.L. Yola, T. Eren, N. Atar, Sensors and Actuators B: Chemical 218 (2015) 215.
- V.K. Gupta, M.L. Yola, T. Eren, F. Kartal, M.O. Çağlayan, N. Atar, *Journal of Molecular Liquids* 190 (2014) 133.
- 28. V.K. Gupta, N. Atar, M.L. Yola, C. Darcan, Ö. Idil, Z. Üstündağ, Suhas, *Journal of Molecular Liquids* 188 (2013) 81.
- 29. V.K. Gupta, T. Eren, N. Atar, M.L. Yola, C. Parlak, H. Karimi-Maleh, *Journal of Molecular Liquids* 208 (2015) 122.
- 30. N. Atar, T. Eren, M.L. Yola, H. Karimi-Maleh, B. Demirdogen, RSC Advances 5 (2015) 26402.
- 31. B.C. Prasongsidh, G.R. Skurray, Food Chemistry 62 (1998) 355.
- 32. Ž. Nikolovska-Čoleska, L. Klisarova, L. Šuturkova, K. Dorevski, Analytical Letters 29 (1996) 97.
- M.L. Yola, N. Atar, Z. Üstündağ, A.O. Solak, *Journal of Electroanalytical Chemistry* 698 (2013)
   9.
- 34. [34] R.S. Nicholson, I. Shain, Analytical Chemistry 36 (1964) 706.
- 35. M.L. Yola, N. Özaltin, Reviews in Analytical Chemistry 30 (2011) 29.
- 36. M.L. Yola, N. Özaltin, Revista de Chimie 62 (2011) 420.

© 2015 The Authors. Published by ESG (<u>www.electrochemsci.org</u>). This article is an open access article distributed under the terms and conditions of the Creative Commons Attribution license (http://creativecommons.org/licenses/by/4.0/).